5-1991

Single-Mode Fiber Microlens with Controllable Spot Size

Chris W. Barnard
University of Ottawa

John W.Y. Lit
Wilfrid Laurier University, jlit@wlu.ca

Single-mode fiber microlens with controllable spot size

Chris W. Barnard and John W. Y. Lit

A novel method for fabricating microlenses on tapered single-mode fibers is shown to be able to control the lens spot size. The fiber cladding is first symmetrically tapered by etching it with an evaporating ammonium bifluoride solution. A hemispheric lens is then melted on the taper tip with a CO_2 laser. The lens can reduce the fiber mode radius to 40% of its original value. A theoretical calculation of the focused spot size agrees well with experimental results. *Key words:* Fiber microlenses, single-mode fiber coupling.

I. Introduction

The coupling loss between a laser diode and a single-mode fiber can limit fiber systems. A major cause of the loss is that the typical spot size of a fiber mode is much greater than that of a laser. Because of the large difference between the numerical apertures of the laser and the fiber, the strongly divergent laser mode does not couple efficiently to the fiber. For example, the spot radius of an InGaAsP laser diode is ~1 μm while the spot radius of a fiber, single-moded at the laser wavelength, is ~5.5 μm.[1] When butt coupling a fiber to a laser these dimensions give a large coupling loss, typically ~10 dB.[2] Coupling single-mode fibers to integrated optical waveguides presents the same problem because the waveguide mode is usually smaller and hence more divergent than the fiber mode.[3]

Single-mode coupling efficiency is maximized by transforming the modes so that they match, i.e., have the same transverse field distribution or in the case of Gaussian beams, the same numerical aperture. The coupling from a laser diode to a fiber, or between a waveguide and a fiber, can be increased by inserting one or more lenses between the laser and the fiber,[1] by fabricating a microlens on the fiber tip,[4] or by appropriately adjusting the waveguide parameters.[5] The various methods of single-mode fiber coupling have been summarized by Neumann,[3] Khoe *et al.*,[6] and Ghafoori-shiraz and Asano.[2]

Fiber microlenses offer some distinct advantages over other coupling techniques. Although the technique of adding lenses between the waveguide and the fiber decreases with alignment sensitivity, it increases the cost, complexity, and size of the device. Microlenses do not involve additional components. Even though it is difficult to control the lens diameter during most fabrication processes, the fabrication is generally simple and fast. Also, when coupling light from a laser diode to a fiber, a microlens can significantly reduce the damaging optical feedback to the laser.[7] The major disadvantage of microlenses is that their coupling efficiency is alignment sensitive.

Microlenses have been fabricated on the ends of single-mode fibers by various methods.[3] Lenses have been attached to the flat end of a fiber by photolithography,[8] by dipping a tapered fiber into molten glass,[9] and by fusing a drop from a silica rod to the fiber end.[10] Another approach is to shape the fiber end by means of chemical etching[2] or polishing.[4] Again, another method is to melt the fiber while pulling it to form a melted taper lens.[7] The best lenses decrease the coupling loss from 7 to 11 dB to <3 dB.[2] With a microlens the lowest reported laser to fiber coupling loss is 1.5 dB.[11]

To date, microlens fabrication procedures cannot produce lenses with a predictable spot size that can be controlled over a wide range. A process, amenable to mass production, is required that can fabricate microlenses with a predictable spot size. To this end, the dependence of the spot size on the lens dimensions must be known and the fabrication process must be able to accurately control the dimensions. In this paper we present a fabrication method for producing a new type of single-mode fiber microlens. Fibers are first tapered by etching the cladding with ammonium bifluoride. A focused CO_2 laser then melts a hemispheric lens on the taper end. The tapering provides a

John Lit is with Wilfrid Laurier University, Department of Physics & Computing, Waterloo, Ontario N2L 3C5, Canada; when this work was done Chris Barnard was with University of Waterloo, Ontario N2L 3G1, Canada; he is now with University of Ottawa, Department of Electrical Engineering, Ottawa, Ontario K1N 6N5, Canada.

Received 13 August 1990.
0003-6935/91/151958-05$05.00/0.

means of controlling the lens diameter and laser melting provides potentially more control over the lens diameter than conventional fiber melting heat sources, such as the electric arc discharge[7] and the microtorch.[12] This process provides a means of controlling the lens radius over a wide range, as opposed to other techniques that have limited ranges, such as selective etching[2] and photolithography.[8] Cladding etching easily produces symmetrical tapers which are essential for distortion free focusing. It is difficult to produce melted tapers that are symmetrical.[6] It is also difficult to predict the spot size of a melted taper lens[13] because the mode transformation due to the tapered core is difficult to characterize. Tapering only the cladding does not affect the mode in the fiber nearly as much and therefore facilitates the prediction of the lens spot size.

II. Analysis of Lenses on Tapered Cladding Fibers

A hemispheric lens on a cladding tapered fiber is shown in Fig. 1. By approximating the fundamental fiber mode with a Gaussian radial distribution[14] the focusing of a microlens can be found from Gaussian optics.[15] The spot size (radius of the waist) w_f of a lens of focal length f is given by

$$w_f^2 = \frac{w_L^2}{1 + \left[\frac{\pi w_L^2}{\lambda}\right]^2 \left[\frac{1}{f} - \frac{n}{R_L}\right]^2}, \tag{1}$$

where λ is the free space wavelength, w_L is the Gaussian beam radius at the lens, and R_L is the radius of curvature of the wavefront at the lens. The focal length of a melted fiber lens is given by

$$f = \frac{r}{(n-1)}, \tag{2}$$

where r is the lens radius and n is the fiber refractive index. If the beam waist is at the lens, $R_L = \infty$, which is equivalent to having an incident plane wave. In this case

$$w_f^2 = \frac{w_L^2}{1 + \left[\frac{\pi w_L^2}{f\lambda}\right]^2}. \tag{3}$$

Note that a beam with its waist at the lens will have a larger spot size than a contracting beam ($R_L < 0$) and a smaller spot size than an expanding beam ($R_L > 0$) (with the same w_L). The wavefront in an untapered fiber has a phase front of infinite curvature so it propagates as a plane wave. In this case Eq. (3) is used to calculate the fiber lens spot size. If tapering the fiber causes the mode to expand or contract, R_L is finite and Eq. (1) should be used to accurately calculate the lens spot size unless $R_L \gg nf$. Usually R_L is difficult to determine so Eq. (3) is used as an approximation.

For step index fibers mode radius w_L, defined as the radial distance at which the field amplitude is e^{-1} of its maximum, can be approximated by[14]

$$\frac{w_L}{a} = 0.65 + \frac{1.619}{V^{3/2}} + \frac{2.879}{V^6}. \tag{4}$$

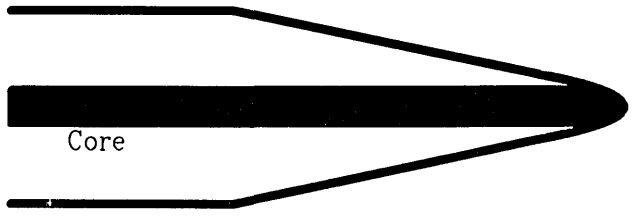

Fig. 1. Tapered cladding lens.

The term V is defined by

$$V = \frac{2\pi a}{\lambda}[n_1^2 - n_2^2]^{1/2}, \tag{5}$$

where a is the core radius, and n_1 and n_2 are the core and cladding refractive indices. The fiber mode radius depends strongly on the core radius a, since it appears in both Eqs. (4) and (5). For a melted taper this means that as the mode propagates down the taper it will spread into the cladding and couple to the cladding guided modes. Because of this, it is difficult to predict w_L for a melted taper lens. Also note that, since the mode is expanding, the factor R_L in Eq. (1) must be taken into account when calculating the spot size of a lens on a melted taper. Therefore, predicting the spot size of a lens on a tapered cladding fiber is easier and more accurate than for a tapered core fiber.

In a fiber which has only its cladding tapered, the mode is unaffected by the tapering, except at the extreme end of the taper. The only complication arises for a lens with a very small radius which will have a thin cladding before the lens. For ordinary telecommunication fibers, if the cladding radius becomes less than approximately twice the core radius, the mode will be affected since the evanescent field amplitude will be significant at the cladding–air boundary. In this case the larger refractive index difference between the cladding and the air will cause the evanescent field to fall off sharply so that the mode contracts along the taper. Thus, calculation of the mode radius becomes more complicated since the solution for a step index fiber assumes an infinite cladding. At the end of the taper we assume that the core–cladding refractive index difference is insignificant compared to the core–air index difference. The mode radius is then calculated from Eqs. (4) and (5) by substituting the cladding radius for a, the core refractive index for n_1, and 1 for n_2. The mode radius calculated in this manner decreases along the taper so that it is smaller than the original mode radius at the point where the cladding has been completely removed. The mode radius at a given point of the taper is taken as the smaller value of the original mode radius and the value calculated for the end of the taper. Note that at the beginning of the taper the mode is guided by the core–cladding boundary and at the end of the taper the mode, which has contracted, is guided by the core–air boundary.

Once the mode radius at the lens is calculated, Eq. (3) is used to calculate the lens spot size, assuming that the lens diameter is equal to the fiber diameter just before the lens. Since the rate of contraction of the

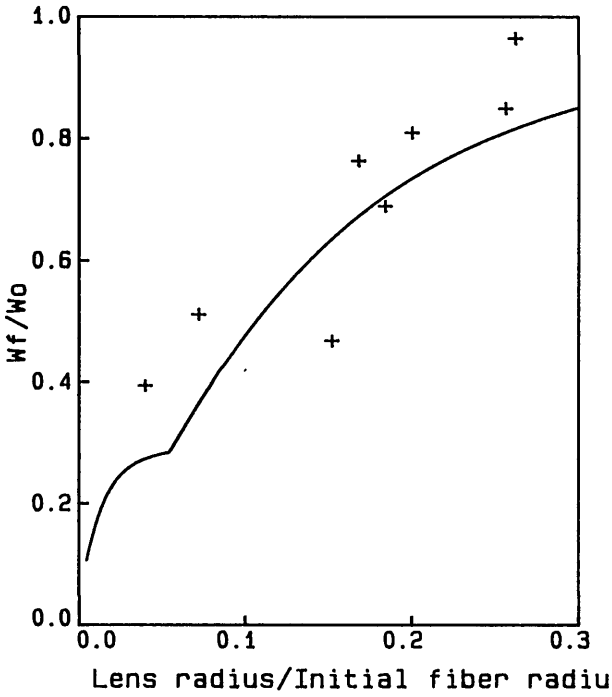

Fig. 2. Theoretical spot size of etched tapered cladding lens vs lens radius with the measured spot sizes.

mode is much smaller than for a tapered core fiber, Eq. (3) will give more accurate results for a lens on a tapered cladding fiber. Equation (3) can be used to estimate the lens spot size as long as $R_L \gg nf$.

Using the parameters of the experimental (noncommunication) fibers ($n_1 = 1.4575$, $n_2 = 1.453$, cladding diameter = 125 μm, $a = 2.05$ μm, and $w_0 = 2.31$ μm at 633 nm) the calculated spot size from Eq. (3) is given by the curve in Fig. 2 (w_0 is the original fiber mode size). The kink in the curve corresponds to the point where the cladding has become thin enough so that the mode extends significantly to the air boundary as discussed above. To the left of the kink the mode will be contracting so that the spot size will be smaller than that calculated from Eq. (3).

III. Fabrication Procedure

Optical fibers have been etched by solutions of hydrofluoric acid for various purposes, such as to produce biconical tapers used for fiber sensors.[16] When a silica fiber end is dipped into a hydrofluoric acid solution the etching rate of the boron doped core is slower than that of the cladding.[2,12] As a result, the flat fiber end develops a small conical protuberance that is centered on the fiber face. The diameter of the base of the circular cone is equal to the core diameter, and the height of the cone depends on the acid concentration. This cone can then be flame polished to form a microlens, of a diameter equal to the core diameter, that protrudes from the flat end of the fiber.[12]

In our method, ammonium bifluoride (AB) was used as the etching solution. Figure 3 shows how evaporation of the solution during the etching process tapers

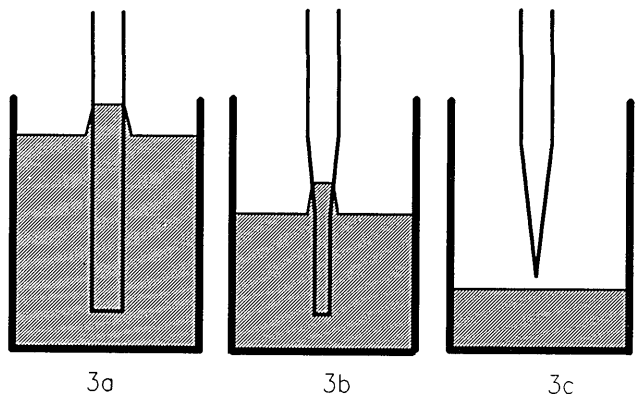

Fig. 3. Formation of a cladding tapered fiber from etching the fiber in an evaporating ammonium bifluoride solution.

the fibers naturally. Figure 3(a) shows a fiber end after it has just been dipped into an AB solution. After about an hour the solution evaporated slightly [Fig. 3(b)]. Because the fluid level slowly drops, the amount that the fiber is etched increases toward the end of the fiber. Thus, the amount of time for which a section of the fiber is etched is controlled by the rate of evaporation. Figure 3(c) shows the taper after the solution has dropped below the end of the fiber.

For our container and overlying atmosphere the acid evaporated at a rate of ~3 μm/min and the etching rate (rate of radius decrease) depended linearly on the AB concentration C as

$$\frac{dr}{dt}\ (\mu\text{m/min}) = -0.52C\ (\text{g/mliter}). \tag{6}$$

AB dissolved in water in room temperature saturates at a concentration of between 0.75 and 0.91 g/mliter so the maximum achievable etching rate is ~0.4 μm/min. The taper angle, and the corresponding length, can be controlled by adjusting the solution concentration with the saturation point of the solution limiting the largest possible taper angle.

This method of fabricating fiber tapers gives good control over the fiber radius at the end of the taper as well as the taper angle. The resulting tapers were symmetrical and the taper shapes could be easily reproduced. We found that there was no detectable difference between the shapes of two tapers deposited for equal lengths of time in the same solution. Many tapers of a similar shape can be made simultaneously so this process can be easily adapted to mass production.

The surface of the etched area of the fiber was quite rough with a frosted appearance. The surface at the taper end was not as rough as the surface at the taper beginning. The frosted area extended, on some fibers, several millimeters above the watermark. It is believed that this frostiness is caused by acid being drawn up by surface tension and not by the solution vapor, because a fiber suspended above the solution was not frosted as the immersed fibers were. Because of this, the roughness of the surface is believed to be caused by

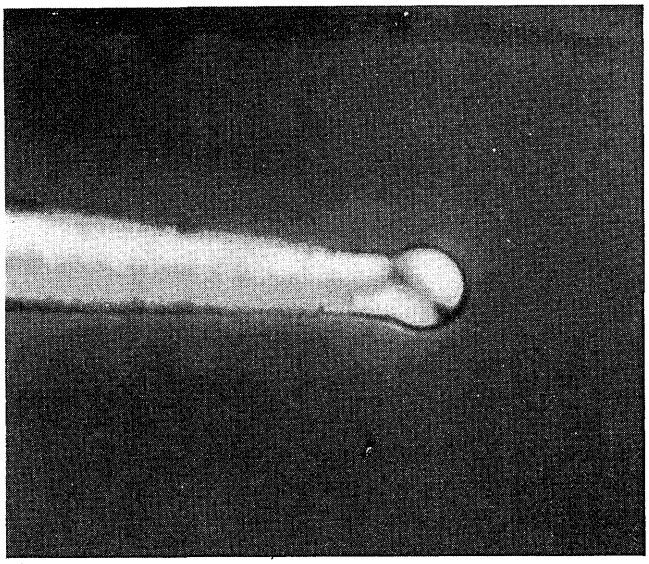

Fig. 4. Microlens melted on an etched taper (320×); lens diameter = 35 μm.

the different evaporation rates of acid droplets on the fiber surface above the solution.

Lenses are melted on the ends of a taper by slowly moving it toward a focused CO_2 laser spot until it starts to melt. The fiber is threaded through a needle used to position the fiber with respect to a laser beam. A He–Ne laser is coupled into the opposite end of the fiber and its output from the microlens is used for monitoring. The fiber, suspended downward, is slowly moved toward the CO_2 laser focal spot until it begins to glow. Since the fiber is suspended vertically, the molten end of the fiber forms a spherical drop that solidifies when the fiber cools. By moving the taper tip toward the focal spot while viewing it with a microscope, the melting of the tip can be stopped when the radius of the spherical drop reaches a desired value. Figure 4 shows a lens melted on the end of an etched taper. This photograph shows how the rough edges created by etching have been smoothed by the melting process so that scattering from the rough, etched surface of the cladding is eliminated. The lens radius of a tapered lens is typically greater than the cladding radius just before the lens. All lenses had the hemispheric shape centered on the taper indicated by the photograph.

IV. Lens Testing

To test Eq. (3), the lens spot sizes were measured and plotted as a function of their radii. The lens spot sizes were measured by the near field scanning technique.[17] A magnified image of the fiber mode was scanned across several planes on either side of the beam waist. The radial intensity dependence of each scan was fit to a Gaussian function to give the mode radius as a function of position z in the direction of propagation. To find the mode radius at waist w_f, mode radius values $w(z)$ were fit to a curve, describing the propagation of a Gaussian beam:

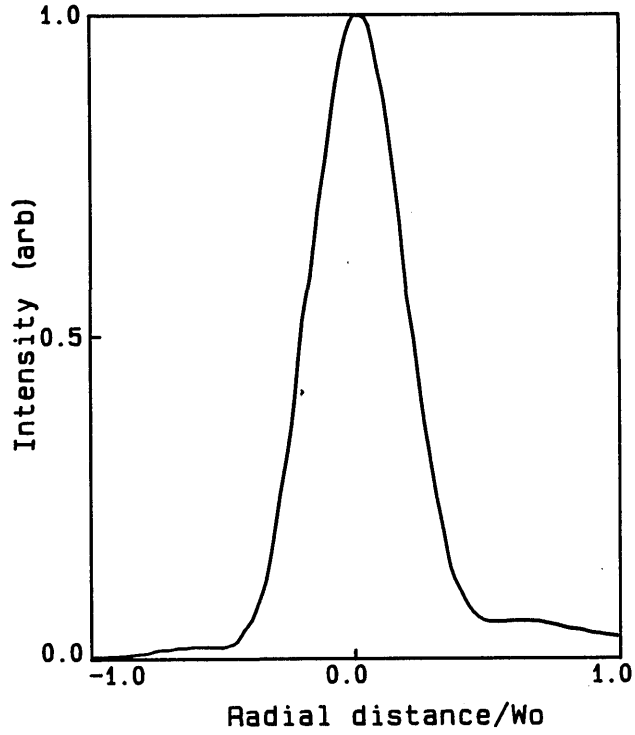

Fig. 5. Near field scan of the focused mode of a microlens. The radial distance is normalized with respect to the initial fiber mode radius.

$$w(z) = w_f\left[1 + \left(\frac{z}{z_f}\right)^2\right]^{1/2}, \tag{7}$$

where $z_f = \pi w_f^2/\lambda$. The typical scan in Fig. 5 shows that the lenses have symmetrical focused spots with negligible secondary diffraction maxima, similar in shape to the fundamental fiber mode.

For comparison with the curve from Eq. (3) the measured spot sizes vs the lens radii are shown in Fig. 2. This figure shows that it is easy to predict the spot radius from the lens radius and that the spot radius can be reduced to less than half of the fiber mode radius.

V. Summary

A novel method of fabricating spherical microlenses on tapered single-mode fibers has been presented. The fabrication process for the etched tapers consistently produced symmetrical tapers with the same shape and taper angle. The final shape of this type of taper can be easily controlled by two parameters: the etching time and the acid concentration. The lens melting procedure is simple, accurate, and shows promise of being able to control the lens diameter. A well-established fabrication process should be able to produce symmetrical, etched taper lenses with a reproducible shape. The experimental spot radii of the etched taper lenses agree quite well with simple theoretical predictions. Since the fiber mode is not transformed by the tapered cladding fiber, it is much easier to estimate the dependence of the spot size on the lens radius than for a melted taper lens with a tapered core.

The smallest demonstrated spot size is ~40% of the original mode radius.

This work was supported by the Natural Sciences & Engineering Research Council of Canada. C. W. B. is supported by an NSERC Canada Postgraduate Scholarship.

References

1. K. Kawano, M. Saruwatari, and O. Mitomi, "A New Confocal Combination Lens Method for a Laser-Diode Module Using a Single-Mode Fiber," IEEE/OSA J. Lightwave Technol. **LT-3,** 739–745 (1985).
2. H. Ghafoori-shiraz and T. Asano, "Microlens for Coupling a Semiconductor Laser to a Single-Mode Fiber," Opt. Lett. **11,** 537–539 (1986).
3. E. G. Newmann, *Single-Mode Fibers* (Springer-Verlag, New York, 1988).
4. H. Sakaguchi, N. Seki, and S. Yamamoto, "Power Coupling from Laser Diodes into Single-Mode Fibres with Quadrangular Pyramid-Shaped Hemiellipsoidal Ends," Electron. Lett. **17,** 425–426 (1981).
5. J. Albert and G. L. Yip, "Insertion Loss Reduction Between Single-Mode Fibers and Diffused Channel Waveguides," Appl. Opt. **27,** 4837–4843 (1988).
6. G. D. Khoe, J. Poulissen, and H. M. De Vrieze, "Efficient Coupling of Laser Diodes to Tapered Monomode Fibres with High-Index End," Electron. Lett. **19,** 205–206 (1983).
7. T. Schwander, B. Schwaderer, and H. Storm, "Coupling of Lasers to Single-Mode Fibres with High Efficiency and Low Optical Feedback," Electron. Lett. **21,** 287–289 (1985).
8. P. D. Bear, "Microlenses for Coupling Single-Mode Fibers to Single-Mode Thin-Film Waveguides," Appl. Opt. **19,** 2906–2909 (1980).
9. G. D. Khoe, H. G. Kock, D. Kuppers, J. H. F. M. Poulissen, and H. M. De Vrieze, "Progress in Monomode Optical-Fiber Interconnection Devices," IEEE/OSA J. Lightwave Technol. **LT-2,** 217–227 (1984).
10. J. Yamada, Y. Murakami, J. Sakai, and T. Kimura, "Characteristics of a Hemispherical Microlens for Coupling Between a Semiconductor Laser and Single-Mode Fiber," IEEE J. Quantum Electron. **QE-16,** 1067–1072 (1980).
11. W. Bludau and R. H. Rossberg, "Low-Loss Laser-to-Fiber Coupling with Negligible Optical Feedback," IEEE/OSA J. Lightwave Technol. **LT-3,** 294–302 (1985).
12. M. Kawachi and T. Edahiro, "Microlens Formation on VAD Single-Mode Fibre Ends," Electron. Lett. **18,** 71–72 (1982).
13. R. Keil, E. Klement, K. Mathyssek, and J. Wittmann, "Experimental Investigation of the Beam Spot Size Radius in Single-Mode Fiber Tapers," Electron. Lett. **20,** 621–622 (1984).
14. D. Marcuse, "Loss Analysis of Single-Mode Fiber Splices," Bell Syst. Tech. J. **56,** 703–718 (1977).
15. A. Gerrard and J. M. Burch, *Introduction to Matrix Methods in Optics* (Wiley, Toronto, 1975), pp. 26–35, 76–81, 116–119.
16. C. A. Villarruel, D. D. Dominguez, and A. Dandridhe, "Evanescent Wave Fiber Optic Chemical Sensor," Proc. Soc. Photo-Opt. Instrum. Eng. **798,** 225–229 (1987).
17. D. W. Hewak and J. W. Y. Lit, "Solution Deposited Optical Waveguide Lens," Appl. Opt. **28,** 4190–4198 (1989).